

1 Aerosol trace element solubility and deposition fluxes over the ~~polluted, dusty~~ Mediterranean and
2 Black Sea basins

3 Rachel U. Shelley ¹, Alex R. Baker ¹, Max Thomas ^{1,2}, Sam Murphy ^{1,3}

4

5 1 – Centre for Ocean and Atmospheric Sciences, School of Environmental Sciences, University of East
6 Anglia, Norwich, NR4 7TJ, UK

7 2 – now at: Met Office Hadley Centre, Exeter, EX1 3PB, UK

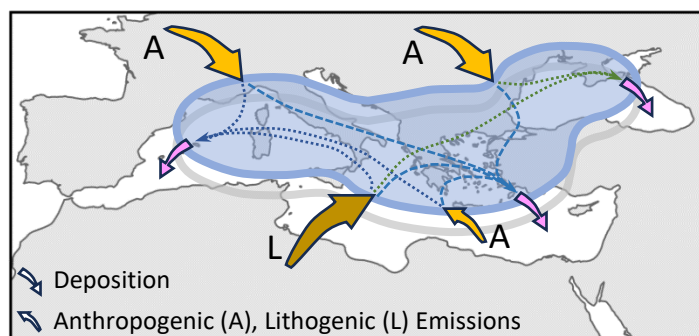
8 3 – now at: Hydrock now Stantec, Merchants' House North, Wapping Road, Bristol, BS1 4RW, UK

9

10 **Abstract**

11 Aerosol samples collected during summer 2013 on GEOTRACES cruise GA04 in the Mediterranean
12 and Black seas were analysed for their soluble and total metal and major ion composition. The
13 fractional solubilities (soluble / total concentrations) of the lithogenic elements (Al, Ti, Mn, Fe, Co,
14 Th) varied strongly with atmospheric dust loading. Solubilities of these elements in samples that
15 contained high concentrations of mineral dust were noticeably lower than at equivalent dust
16 concentrations over the Atlantic Ocean. This behaviour probably reflects the distinct transport and
17 pollutant regimes of the Mediterranean basin. Elements with more intense anthropogenic sources
18 (P, V, Ni, Cu, Zn, Cd, Pb) had a variety of largely independent sources in the region and generally
19 displayed higher fractional solubilities than the lithogenic elements. Calculated dry deposition fluxes
20 showed a west to east decline in the N/P ratio in deposition over the Mediterranean, a factor that
21 contributes to the P-limited status of the eastern basin. Atmospheric deposition may make a
22 significant contribution to the surface water budgets of Mn and Zn in the western Mediterranean.

23



24

25 **1 Introduction**

26 Aerosols have both direct and indirect impacts on the global climate system (e.g. Martin, 1990;
27 Carslaw et al., 2010). Aerosols directly interact with incoming and outgoing solar radiation and act as
28 seeds for cloud formation. Indirectly, they impact the climate through the deposition of both
29 essential and potentially toxic elements to aquatic and terrestrial ecosystems, where they can be
30 assimilated by photosynthetic microbes (Jickells et al., 2005; Jickells and Moore, 2015; Okin et al.,
31 2011; Westberry et al., 2023).

32 Aerosol metals are sourced from natural (mineral dust, sea spray, biomass burning/wildfires,
33 glacial flour, volcanoes, bioaerosols) and anthropogenic (metal smelting, industry, mining, vehicles
34 and shipping) sources, and can be transported vast distances in the atmosphere. In marine
35 environments, sea spray aerosol is often the largest contributor to aerosol mass, especially far from
36 anthropogenic and continental sources (de Leeuw et al., 2011), although mineral dust arguably
37 exerts a greater impact on ecosystem functioning, specifically with respect to the input of
38 biogeochemically important elements (Jickells et al., 2005; Hamilton et al., 2022). In marine regions
39 under the transport pathways of mineral dust from the world's major desert regions, atmospheric
40 deposition is a major external source of macro- (P) and micronutrients (e.g., Fe, Mn, Cu, Zn)
41 (Hamilton et al., 2022).

42 The Mediterranean and Black seas are isolated from the global ocean system: the Mediterranean
43 being connected to the Atlantic Ocean via the Strait of Gibraltar, with the Mediterranean and Black
44 seas connected via the Dardanelles-Sea of Marmara-Bosporus system. During the summer, both seas
45 are highly stratified, largely due to thermal stratification in the Mediterranean and also due to high
46 riverine inputs of fresh water in the Black Sea. Under these conditions, the main external sources of
47 nutrients to the surface waters of both seas are atmospheric and riverine inputs. The Mediterranean
48 is classified as a Low Nutrient Low Chlorophyll (LNLC) ecosystem, characterised by increasing
49 oligotrophy from the western to eastern basins. The Black Sea is the world's largest permanently
50 anoxic marine basin, a status that profoundly shapes its ecosystem functioning. Compared to open-
51 ocean waters, high concentrations of dissolved trace metals (e.g., Al, Mn, Fe, Co, Ni, Cu, Zn, Cd, Pb)
52 are observed in the surface waters of both the Mediterranean and Black seas (Boyle et al., 1985;
53 Guieu et al., 1998; Tovar-Sanchez et al., 2014; Dulaquais et al., 2017; Gerringa et al., 2017; Middag et
54 al., 2022). Both seas are heavily impacted by the atmospheric deposition of natural and
55 anthropogenic material due to their proximity to the Sahara Desert, Europe, and the mega-cities of
56 Cairo and Istanbul (Kubilay et al., 1995; Koçak et al., 2007; Heimbürger et al., 2010; Theodosi et al.,
57 2010b; Theodosi et al., 2013; Kanakidou et al., 2020). Seasonal wildfires (Hernandez et al., 2015) and
58 intense shipping activity in the Mediterranean (Becagli et al., 2012) also add to the aerosol load in
59 the region. In the summer, boundary layer air over the Mediterranean is heavily polluted by
60 anthropogenic sources in Western and Eastern Europe, with occasional incursions of mineral dust
61 from North Africa (Lelieveld et al., 2002; Gkikas et al., 2013). African-origin dust also occasionally
62 reaches the Black Sea in summer (Kubilay et al., 1995).

63 The trace metal composition of aerosols over the Mediterranean has been reported to be
64 dominated by the mixing of these anthropogenic and natural sources (Chester et al., 1981; Chester
65 et al., 1993; Herut et al., 2001). The impact of atmospheric deposition of aerosol-associated
66 elements on the biogeochemistry of the Mediterranean-Black Sea system remains poorly
67 understood (Guieu et al., 2010a; Guieu et al., 2010b), in part because the factors that influence trace
68 element fractional solubility (and hence availability to the microbial community) in this system are
69 unclear. For several dust-borne trace elements (some of which are biogeochemically important, e.g.
70 Fe, Cu) baseline solubility appears to be low but increases during atmospheric transport (Jickells et

71 al., 2016; Shelley et al., 2018), as a result of interactions of mineral dust with acidic gases (SO₂ and
72 NO_x), mixing of dust with trace elements of anthropogenic origin and other processes (Baker and
73 Croot, 2010). These processes are likely to operate rather differently in the Mediterranean / Black
74 Sea atmosphere compared to the relatively well studied Atlantic atmosphere (e.g. Buck et al., 2010;
75 Jickells et al., 2016; Shelley et al., 2018), due to the differences in the relative proportions of dust
76 and anthropogenic emissions and their transport and mixing regimes.

77 In this paper, we discuss data for a suite of total and soluble elements from aerosols collected
78 during the GEOTRACES cruise, GA04, to the Mediterranean and Black seas. The solubility of trace
79 elements primarily associated with mineral dust (Al, Ti, Mn, Fe, Co, Th) is considered separately from
80 elements whose sources are more closely associated with anthropogenic activities (P, V, Ni, Cu, Zn,
81 Cd, Pb), although individual aerosol samples will contain a mixture of both lithogenic and
82 anthropogenic sources of each element (e.g. Chester et al., 1993). The potential influences on the
83 solubility of these elements in the unusual conditions of the Mediterranean / Black Sea atmosphere,
84 where the surrounding land masses contain significant sources of mineral dust and anthropogenic
85 pollutants is discussed. The potential impact of atmospheric deposition on surface water
86 macronutrient (N/P) status and dissolved metal budgets of the Mediterranean Sea is also
87 considered.

88

89 **2 Methods**

90 *2.1 Study region*

91 Aerosol samples were collected during the GEOTRACES cruise GA04 aboard the RV *Pelagia* during
92 May-August 2013 (Table 1, Fig. 1). A full description of the Mediterranean, Aegean and Sea of
93 Marmara sections of the cruise track (Legs 1 and 3) has previously been published (Rolison et al.,
94 2015; Dulaquais et al., 2017; Gerringa et al., 2017; Middag et al., 2022).

95

96 Table 1. Summary of the GA04 cruise legs, dates in 2013 and sample numbers.

	Cruise Leg	Dates	Samples
Leg 1	Southern leg, Lisbon – Istanbul	16 May – 4 June	01 – 18
Leg 2	Black Sea, Istanbul – Istanbul	14 - 22 July	19 - 25
Leg 3	Northern leg, Istanbul – Lisbon	26 July – 10 August	26 - 40

97

98 *2.2 Sample collection*

99 Two high volume, mass flow controlled, Total Suspended Particulate aerosol samplers (Tisch
100 Environmental, Ohio, USA) were located on the wheelhouse roof. Samples were collected on
101 Whatman 41 (W41) filter sheets (203 x 254 mm, cellulose). For trace metals (TM), filters were acid
102 washed before use (0.5 M HCl and 0.1 M HNO₃; Baker et al., 2007), while for major ions (MI), filters
103 were used without pre-treatment. The aerosol samplers were automatically controlled to operate
104 during relative (from the ship's bow) wind directions of between -80 ° and 145 ° and at wind speeds
105 > 2 m s⁻¹ to minimise the risk of contamination from the ship's exhaust (Chance et al., 2015). TM and
106 MI samples were generally collected in pairs, although the MI sampler malfunctioned during Leg 2.
107 No MI data are available for this section of GA04. Samples were collected over ~24 h periods, with
108 the exception of sample TM19 which ran for 46 h. Three types of filter blanks were collected: 1)

109 cassette blank – filter placed in filter cassette and stored in a plastic bag for 24 h, 2) process blank –
110 filter placed in filter cassette and placed in the aerosol sampler and left for 24 h without the motor
111 running, 3) motor blank – filter placed in filter cassette and placed in the aerosol sampler with the
112 motor running for 5 min. Upon collection, all filter samples were folded inwards, zip-lock bagged and
113 stored frozen (-20 °C) onboard the ship. Samples and blanks remained frozen in the home laboratory
114 until either strong acid digestion (total trace metals) or leaching for soluble trace metals or major
115 ions. Reagent blanks were also taken to monitor for potential contamination arising from the
116 digestion or leaching processes. Where blanks were above the analytical limit of detection for an
117 analyte, these were averaged and subtracted from the results obtained for the samples. If blanks
118 were below the limit of detection no blank subtraction was done.

119

120 2.3 Sample analysis

121 2.3.1 Total trace elements (Al, P, Ti, V, Mn, Fe, Co, Ni, Cu, Zn, Cd, Pb, Th)

122 One eighth of the TM filter was placed in a 15 mL Teflon vial. Four mL of a 4:1 mixture of
123 ultrapure HNO₃: HF (both Merck, Trace Select Ultra) was pipetted in, and the vial capped. The
124 samples were digested using a microwave system (Milestone UltraWave) using the silica sand pre-
125 programmed method (T = 240 °C, P = 110 bar). Following the digestion, the solutions were
126 transferred to clean Teflon vials and taken to near-dryness on a Teflon-coated hotplate. The hotplate
127 was housed in a fume cupboard, inside a plastic box, from which acid fumes were drawn through a
128 saturated solution of CaCO₃ in order to remove excess HF (Baker et al., 2020). The residue was then
129 redissolved in 0.48 M HNO₃ (Shelley et al., 2015; Shelley et al., 2017). All samples and blanks were
130 subsequently spiked with 10 ppb Rh as an internal standard. Aluminium, Fe and P were determined
131 by ICP-AES (Thermo Scientific i-CAP PRO). All other elements (Ti, V, Mn, Co, Ni, Cu, Zn, Cd, Pb, Th)
132 were determined by ICP-MS (Thermo Scientific, iCAP TQ) and calibrated using external standards
133 (SPEX CertiPrep). Calibrations were verified by analysis of matrix reference materials (MRMs TM-
134 27.3, TMDA-64.2, TM-27.4 and TMDA-62.3; Environment Canada) with recoveries being within 5%
135 (Al, Ti, V, Mn, Fe, Zn), 10% (Co, Ni, Cd) and 15% (Cu, Pb) of certified values. Aliquots of Arizona Test
136 Dust were also digested alongside aerosol samples. The results obtained are summarised in Table S1.
137 Total Cr, As, Sb, Ba, La, Ce, Nd and U were also determined but are not discussed here as there are
138 no corresponding soluble metal data for these elements.

139

140 2.3.2 Soluble trace elements (Al, Ti, V, Mn, Fe, Co, Ni, Cu, Zn, Cd, Pb, Th)

141 One quarter of each TM filter was leached for 1-2 h with ammonium acetate buffered to pH 4.7,
142 with occasional gentle shaking by hand. The resulting leachate was filtered using 0.2 µm pore sized
143 cellulose acetate syringe filters (minisart, Sartorius) (Baker et al., 2007). The samples were analysed
144 by ICP-AES (Varian Vista Pro, Fe, Al, Mn, Ti, Zn, V) and ICP-MS (Thermo X-Series; Cu, Ni, Co, Cd, Pb,
145 Th). Calibrations were prepared from external standards (SPEX CertiPrep) and recoveries for MRMs
146 (TM-27.3, TMDA-64.2; Environment Canada) were within 5% (Ti, Mn, Fe, Co, Ni, Cu, Pb), 10% (Al, V,
147 Zn) and 25% (Cd) of certified values.

148

149 2.3.3 Soluble major ions (Na⁺, NH₄⁺, Mg²⁺, K⁺, Ca²⁺, Cl⁻, NO₃⁻, SO₄²⁻, Br⁻, C₂O₄²⁻) and soluble phosphate

150 One quarter of each MI filter was leached using ultrahigh purity water (18.2 MΩ.cm) with
151 ultrasonic agitation for 1 hour (Baker et al., 2007). After filtration (0.2 μm), samples were analysed
152 using a Dionex ICS-5000 dual channel ion chromatograph equipped with CS12A and AS18 columns
153 for cation and anion separation, respectively. Calibration standards were prepared from analytical
154 grade salts (Fisher Scientific) of the ions and verified against MRMs (ION-915 and KEJIM-02;
155 Environment Canada). Recoveries for these MRMs were within 5% (Na⁺, Mg²⁺, Ca²⁺, Cl⁻, NO₃⁻, SO₄²⁻)
156 and 10% (K⁺) of their certified values. For soluble phosphate determination, one eighth of each MI
157 filter was leached using 1 mM NaHCO₃, also using 1 hour of ultrasonic agitation. Soluble reactive
158 phosphorus (hereafter referred to as phosphate) was determined in the filtered leachates by
159 spectrophotometry (Baker et al., 2007).

160

161 *2.4 Calculation of derived parameters*

162 Fractional solubility was calculated as the ratio s-X / t-X, expressed as a percentage, where s-X
163 and t-X are the soluble and total concentrations respectively for each trace element (X).

164 Enrichment factors (EF) were calculated using the elemental ratios of the element of interest (X)
165 and Al (as the lithogenic tracer) in aerosol with respect to the X/Al ratio in shale (Turekian and
166 Wedepohl, 1961), according to: $EF = ([X]_{aero}/[Al]_{aero})/([X]_{shale}/[Al]_{shale})$. Elements of predominantly
167 lithogenic origin are not expected to be enriched and to have EFs close to 1. As there is natural
168 variability in the abundances of elements in crustal material, we only consider EFs > 10 as
169 significantly enriched, with other (e.g. anthropogenic) sources of these elements dominating over
170 lithogenic sources.

171 The non-seasalt (nss) component of MI concentrations were calculated by subtracting the
172 contribution of the ion arising directly from seaspray aerosol from the measured concentration (nss-
173 MI = [MI_{aero}] - [MI_{ss}]). Seaspray aerosol contributions were estimated from measured aerosol Na⁺,
174 assuming that the ratio of the ion to Na⁺ in seaspray is identical to that of bulk seawater (Baker et al.,
175 2007).

176

177 *2.5 Dry deposition fluxes*

178 The dry deposition flux (F) was calculated from the product of the concentration of that element
179 (C_x) and a deposition velocity (v_d); $F = C_x * v_d$. Because it is not possible to accurately determine the
180 deposition velocity over the ocean, there is large (a factor of 2-3) uncertainty associated with the v_d
181 term (Duce et al., 1991). For our flux calculations, we used v_d values of 1 cm s⁻¹ for the lithogenic
182 elements and 0.1 cm s⁻¹ for the anthropogenic elements, in order to reflect the size distribution of
183 the particles where these elements are found (Duce et al., 1991). When estimating deposition to the
184 Mediterranean basin we assumed its surface area to be 2.5 x 10⁶ km², and the relative areas of the
185 western and eastern basins to be 1:2. Mineral dust deposition fluxes were estimated from t-Al,
186 assuming that Al is 8 weight percent of dust (Turekian and Wedepohl, 1961).

187

188 *2.6 Air mass back trajectories*

189 Five-day air mass back trajectory (AMBT) simulations were produced using the NOAA Air
190 Resources Laboratory's HYPLIT model (https://www.ready.noaa.gov/HYSPLIT_traj.php) with
191 NCEP/NCAR Reanalysis Project datasets (Stein et al., 2015). Trajectories were calculated for arrival

192 heights of 10, 500 and 1000 m above mean sea level at 3 hourly intervals along the ship's track.
193 Based on the AMBTs, samples were assigned to one of five air mass types, indicative of likely aerosol
194 source characteristics as described below. [Assignments were done principally based on the surface](#)
195 [level \(10 m\) trajectories. However, higher altitude transport \(up to 3000 m\) can be significant for](#)
196 [Saharan dust over the Mediterranean](#) (Scerri et al., 2016), [so upper levels were also considered in](#)
197 [the context of transport from North Africa.](#)

198

199 **3 Results and Discussion**

200 **3.1 Air mass origins during GA04**

201 Example AMBTs and air mass type assignments are shown in Fig. 2 [\(and in more detail in Fig. S1\)](#).
202 Many of the air masses encountered during GA04 arrived at the ship from a north-westerly
203 direction, having passed over continental Europe. We divided these European air masses into two
204 categories. The Eastern European (EEU, n = 15) group had most recently been in contact with Europe
205 to the east and north of the Adriatic Sea, while the Western European (WEU, n = 10) group includes
206 arrivals most recently in contact with mainland Italy, France and the Iberian Peninsula. The
207 Mediterranean (MED, n = 4) and Remote North Atlantic (RNA, n = 3) groups had not interacted with
208 continental land masses within the five days of the simulation (although MED trajectories that
209 passed over islands were not uncommon and for RNA sample TM03 trajectories passed briefly over
210 southwestern regions of Iberia: [see Fig. S1](#)). Eight samples were affected by air mass arrivals from
211 North African (NAF). As illustrated in Fig. 2, trajectories for this group passed over regions identified
212 as potential source areas (PSAs) for dust aerosols, notably the 'Libya/Egypt' and 'Libya/Algeria/Mali'
213 PSAs (Guinoiseau et al., 2022), [but we do not attempt to assign potential dust sources for individual](#)
214 [samples. All of the NAF samples showed the orange colouration associated with desert dust.](#)

215

216 **3.2 Total lithogenic elements (t-Al, Ti, Mn, Fe, Co, Th)**

217 For all the primarily lithogenic elements, the influence of Saharan dust (NAF air mass type) on the
218 aerosol total metal concentrations is clearly visible in samples TM8-14 (Fig. 3, [Table S2](#)). The NAF
219 samples had an orange colour, typical of aerosols with Saharan origin, and all of the lithogenic
220 elements had their maximum concentrations within this air mass type. Molar ratios to Al for these
221 elements ([Table S3](#)) were reasonably consistent across the GA04 Mediterranean-Black Sea air mass
222 types and with their ratios reported in Saharan aerosols collected over the tropical North Atlantic
223 (Shelley et al., 2015; Jickells et al., 2016) and in the eastern Mediterranean (Herut et al., 2016). As
224 expected for elements from primarily crustal sources, no significant enrichment was observed (i.e.
225 $EF \sim 1$) for the lithogenic elements, for all air mass types. (Very similar behaviour was also observed
226 for Ba, La, Ce, Nd and U during GA04 ([Fig. S2](#))). In a few cases EFs for Mn and Co were >3 in European
227 air masses (Fig. 3c & e), but Co was the only lithogenic element to be notably enriched ($EF >10$) in
228 samples (TM03 and 04) whose trajectories passed over the southern tip of Iberia. Lithogenic
229 element concentrations and EF values from GA04 are consistent with previous observations from
230 shipboard sampling (Tables S4 & S5; Chester et al., 1993; Chester et al., 1984; Moreno et al., 2010;
231 Hacısalihoglu et al., 1992; Kubilay et al., 1995) and at a number of coastal and island time series sites
232 (e.g. Kubilay and Saydam, 1995; Koçak et al., 2007; Guieu et al., 2010b; Heimbürger et al., 2010).

233

234 **3.3 Soluble lithogenic elements (s-Al, Ti, Mn, Fe, Co, Th)**

235 In contrast to the total metal concentrations, the highest soluble concentrations for the
236 lithogenic elements were not found in samples from NAF air masses. For example, [median s-Fe](#)
237 [concentrations in aerosols of the Mediterranean and European air mass types \(110, 320 and 180](#)
238 [pmol m⁻³ for MED, WEU, EEU types respectively\) were all considerably higher than in NAF aerosols](#)
239 [\(54 pmol m⁻³\)](#) during GA04. The median s-Fe concentration in the RNA air mass was ~30 pmol m⁻³,
240 similar to the value previously reported for this air mass type in the remote Atlantic: ~15 pmol m⁻³
241 (Baker and Jickells, 2017). This was probably a result of the lower fractional solubility of the
242 lithogenic elements in mineral dust compared to aerosols from other sources (Fig. 4 and Jickells et
243 al., 2016; Shelley et al., 2018) combined with higher fractional solubility of these elements in
244 anthropogenic sources [\(e.g. median fractional solubilities for Fe in the NAF, MED, WEU, EEU and](#)
245 [RNA types during GA04 were 0.4, 2.9, 12.4, 2.8 and 5.1 %, respectively\)](#) and the relatively high
246 (compared to the atmosphere over the North Atlantic) concentration of anthropogenic aerosols
247 encountered during GA04. A common feature of the soluble lithogenic elements during GA04 was
248 the two peaks in concentration in samples TM18 (Sea of Marmara) and TM20 (SW Black Sea), both
249 from EEU air masses, which corresponded with peaks in fractional solubility (Fig. 4).

250

251 **3.4 Total anthropogenic elements (t-P, V, Ni, Cu, Zn, Cd, Pb)**

252 In contrast to the lithogenic elements, the distributions of the anthropogenic elements during
253 GA04 were more diverse (e.g. they had different concentration profiles along the cruise track and in
254 most cases their highest concentrations were not associated with the NAF samples, Fig. 5). All of the
255 anthropogenic elements displayed significant enrichment (EF >10) relative to crustal material,
256 although enrichments were lowest, and in some cases (e.g. for t-V and t-Ni) close to 1, for the NAF
257 samples. These distributions are consistent with these elements having a variety of disparate
258 sources around the region (Pacyna and Pacyna, 2001), which are mixed with mineral dust to varying
259 degrees during atmospheric transport (Chester et al., 1993). EF values for V and Ni were > 10 in
260 many non-NAF samples in the Mediterranean, consistent with shipping being a significant source of
261 these elements (Becagli et al., 2012) but were also close to 1 in samples collected in the Black Sea,
262 where shipping density is lower than in the Mediterranean. Although t-P was not notably enriched in
263 NAF samples (EF values 1.6 – 6.2), we have grouped it with the anthropogenic elements as many
264 samples from other air mass types had EFs >10, suggesting that P (as well as V, Ni, Cu, Zn and Pb) has
265 important non-natural dust sources [\(note that Mahowald et al. \(2008\) suggest that P enrichment](#)
266 [might occur through the uplift of artificially fertilized soils\)](#).

267 Elemental ratios for the anthropogenic elements (Table S3) varied substantially between the
268 different air masses encountered during GA04 as well as between reported values for the northeast
269 Atlantic and eastern Mediterranean (Shelley et al., 2015; Herut et al., 2016). Relative to data
270 collected in earlier decades (late 1970s to early 1990s), there has been a substantial decrease in
271 concentrations and EF values for some elements (especially Pb, Cd) in both the Mediterranean and
272 Black seas (Tables S4 & S5) due to the removal of Pb from petrol and other changes in anthropogenic
273 emissions. However, EF values for Pb during GA04 were roughly an order of magnitude higher than
274 values reported over the eastern tropical Atlantic in the early 2010s (1.8 – 15; Bridgestock et al.,
275 2016) suggesting that the Mediterranean and Black Sea atmosphere [were](#) still subject to significant
276 anthropogenic emissions of Pb [in 2013](#).

277

278 **3.5 Soluble anthropogenic elements (s-V, Ni, Cu, Zn, Cd, Pb) and phosphate**

279 As with the lithogenic elements, concentrations of the soluble anthropogenic elements were
280 lowest in the RNA samples during GA04, with most concentrations being below the limit of detection
281 in that air mass type (Fig. 6). The profiles in Fig. 6 indicate relatively localised, independent sources
282 for s-V, Ni, Cu, Zn, Cd, Pb and phosphate, although there are some common features between the
283 elements. Most elements had relatively high concentrations in the northern Aegean Sea and Sea of
284 Marmara (sample TM18). Soluble Cu, Cd and Pb had relatively high and increasing concentrations
285 towards the end of the cruise near the Iberian Peninsula. Soluble (and total) V and Ni concentrations
286 were strongly correlated ($r^2 = 0.973$ (soluble) and $r^2 = 0.955$ (total), both $p = \ll 0.01$). [V and Ni in
287 aerosols at Lampedusa in the central Mediterranean being primarily attributed to shipping emissions](#)
288 (Becagli et al., 2012), [this](#) is consistent with [the idea that these emissions are the dominant factor
289 controlling s-V and s-Ni concentrations, as previously observed in the Atlantic Ocean](#) (Baker and
290 Jickells, 2017).

291 Fractional solubilities for the anthropogenic elements were generally higher than those of the
292 lithogenic elements, with most values being > 10 %. In contrast to the lithogenic elements, lowest
293 fractional solubilities were not observed in the NAF samples even though EF values indicated that
294 Saharan dust dominated the total element concentrations in these samples (Fig. 5). Phosphate was a
295 possible exception to this with fractional solubilities of 6-36% in NAF samples, < 9% in RNA samples
296 and a range of 14-49% in all other air mass types (Fig 6a).

297

298 3.6 Influences on (lithogenic) element solubility

299 During GA04, all the primarily lithogenic elements (Al, Ti, Mn, Fe, Co, Th) displayed inverse
300 relationships between their total concentrations and fractional solubility (Fig. 7a, c, e, g, i & k). For
301 some elements this is consistent with previously published studies. For instance, similar trends have
302 been observed for Fe in a variety of global settings (Baker et al., 2006; Sholkovitz et al., 2009; Kumar
303 and Sarin, 2010; Sholkovitz et al., 2012; Jickells et al., 2016; Shelley et al., 2018), [including the
304 eastern Mediterranean](#) (Theodosi et al., 2010a), and for Al and Ti in the Atlantic Ocean (Jickells et al.,
305 2016; Shelley et al., 2018; Baker et al., 2020).

306 With the exception of Ti, the solubilities of the lithogenic elements during GA04 differ markedly
307 from their previously reported behaviour over the Atlantic (see data from Jickells et al., 2016 plotted
308 in Fig. 7). For Al and Fe, it is apparent that the NAF samples have generally lower fractional
309 solubilities than for equivalent total element concentrations of Saharan dust aerosols over the
310 Atlantic, while several of the more polluted (WEU and EEU) samples have higher solubilities than
311 expected from the Atlantic total concentration– solubility relationship. The solubility of Mn in
312 Saharan dust aerosols over the Atlantic has been reported to show little variability with atmospheric
313 loading (Fig. 7e, Jickells et al., 2016; Shelley et al., 2018) and similar relationships have been reported
314 for Co and Th in Saharan dust aerosols (Baker et al., 2020). During GA04, Mn, Co and Th solubility
315 appeared to vary strongly with atmospheric loading. Solubilities for these elements in NAF samples,
316 in particular, were substantially lower than previously observed in Saharan dust aerosols over the
317 Atlantic at equivalent total element concentrations.

318 The elements designated as “anthropogenic” (P, V, Ni, Cu, Zn, Cd, Pb) did not generally show
319 clear trends in fractional solubility with atmospheric loading and their solubilities were more
320 consistent with previous results from the open Atlantic (Fig. 7b, d, f, h, j, l, & m; Jickells et al., 2016;
321 Shelley et al., 2018). For most of these elements, solubilities in NAF samples were similar to those in
322 other air mass types. Since the solubilities of anthropogenic sources of these elements are reported

323 to be high at the point of emission (Desboeufs et al., 2005; Hsu et al., 2005; Li et al., 2022), there is
324 presumably less potential for enhancement of solubility during atmospheric transport as exhibited
325 by the lithogenic elements. Phosphate (P) is the exception to this, as it is the only element from this
326 group to show higher solubility in the GA04 samples than in the Jickells et al. (2016) dataset from the
327 Atlantic, for the dataset as a whole and specifically for the NAF / Saharan samples.

328 A number of mechanisms may potentially contribute to the enhancement of elemental fractional
329 solubility during atmospheric transport (and solubility also varies between potential dust sources
330 regions (Shi et al., 2011)). These mechanisms include chemical alteration by acidic species, change in
331 mineral aerosol particle size (and hence surface area to volume ratio), change in mineralogy (also
332 related to changes in particle size distribution) and photochemical redox change (see, for example,
333 Baker and Croot, 2010). While we are lacking a number of pieces of information (aerosol particle size
334 distributions for trace elements and acidic species, trace element redox states, trace element and
335 acidic species mixing states, dust aerosol mineralogy) that might allow us to investigate these
336 mechanisms in detail, the differences between the solubility behaviour observed during GA04 and
337 that reported for aerosols over the Atlantic can be used to make inferences about the mechanisms
338 of solubility control in the Mediterranean atmosphere.

339 Enhancement of trace element solubility in mineral dust at low pH has been demonstrated in the
340 laboratory (Spokes and Jickells, 1996), inferred from observations of atmospheric aerosols (Fang et
341 al., 2017) and incorporated into atmospheric chemistry models to improve simulations of soluble Fe
342 deposition to the ocean (Myriokefalitakis et al., 2018). Acid species (NO_3^- and nss-SO_4^{2-}) and
343 (alkaline) NH_4^+ concentrations during GA04 were significantly higher (t test, $p < 0.05$) than in
344 equivalent air mass types over the Atlantic Ocean (Jickells et al., 2016; Fig. 8). This is consistent with
345 the more polluted nature of the Mediterranean atmosphere and might be expected to lead to higher
346 acid processing (or depression of acid processing, in the case of NH_4^+) of the NAF samples. However,
347 the ratios of $\text{nss-SO}_4^{2-} / \text{t-Fe}$ in the NAF samples were lower than (but not significantly different to)
348 these ratios in Saharan dust over the Atlantic and there does not appear to be an excess of acidic
349 species to enhance acid processing in this case. Calcite content varies significantly with dust source
350 (generally being higher in sources in the north of the Sahara (Chiapello et al., 1997; Kandler et al.,
351 2007)) and may also impact solubility enhancement through neutralisation of acidity. However,
352 while the $\text{nss-Ca}^{2+} / \text{t-Fe}$ ratio in the NAF samples ($1.4\text{-}10.1 \text{ mol mol}^{-1}$) was relatively high, it was not
353 outside the range of values for this ratio for Saharan dust in the Atlantic dataset ($0.07\text{-}10.8 \text{ mol mol}^{-1}$).
354 Variations in calcite content therefore seem unlikely to account for the observed differences
355 between solubility over the Atlantic and Mediterranean. Enhancement of solubility through acid
356 processing also requires that acidic species are internally mixed with mineral dust (i.e. both
357 contained in the same aerosol particles, as opposed to external mixtures where particles of different
358 composition occupy the same volume of air).

359 Ultimately, solubility enhancement through acid processing is dependent on the pH environment
360 of the aerosol on an individual particle basis. This environment will vary strongly through the aerosol
361 population, due to differences in internal mixing of acidic and alkaline species and trace elements
362 (e.g. with particle size (Fang et al., 2017; Baker et al., 2020)) . Furthermore, changes in the liquid
363 water content of the particles (which is dependent on relative humidity and the hygroscopicity, and
364 hence chemical composition, of the particles in question) can result in dramatic changes in pH, even
365 when acid/alkaline ion balance varies little (Pye et al., 2020; Baker et al., 2021). Information about
366 these factors is not available for the GA04 dataset and the insights provided by the above discussion
367 of ion-solubility relationships are therefore limited.

368 Overall, the low solubility of Al, Mn, Fe, Co and Th in NAF samples (relative to similar samples
369 collected over the Atlantic; Fig. 7) appears to be related to the short atmospheric transport pathway
370 to the Mediterranean. This could lead to lower solubility through reduced internal mixing of acidic
371 species with mineral dust particles (which together with slightly lower ratios of acidic species to
372 lithogenic elements in NAF air masses would lead to lower atmospheric processing of dust particles),
373 and a higher proportion of very large (low solubility) mineral particles relative to dust transported
374 over the Atlantic Ocean. Short atmospheric transport times also reduce the potential for solubility of
375 some elements to be enhanced through photochemical redox changes (e.g. insoluble Fe (III) to
376 soluble Fe (II); Longo et al., 2016), although the very similar solubility behaviour of Fe and Al imply
377 that redox changes are not a major control on Fe solubility (since Al has no redox chemistry). The
378 enhanced solubility of Al, Mn, Fe, Co and Th in EEU and WEU samples (relative to equivalent total
379 element concentrations over the Atlantic) may be due to a combination of both primary
380 anthropogenic emissions of high solubility trace elements and secondary enhancement of solubility
381 during transport to the Mediterranean and Black Sea basins due to atmospheric processing driven by
382 pollutant acidic gases.

383

384 3.7 Dry deposition fluxes

385 Aerosol concentrations measured during GA04 have been used to estimate dry deposition fluxes
386 for total inorganic nitrogen ($\text{NO}_3^- + \text{NH}_4^+$), phosphate, mineral dust and soluble Fe, Mn, Ni, Zn and Cd
387 (Table 2). Dry deposition fluxes for the other soluble trace elements are given in Table S6. This
388 approach provides a snapshot of the dry deposition flux that may not be representative of fluxes
389 over longer timescales. However, our estimates appear broadly comparable with fluxes reported
390 from longer-term sampling around the Mediterranean when annual averages are expressed on a
391 daily basis (e.g. DIN 70-126 $\mu\text{mol m}^{-2} \text{d}^{-1}$ (western basin) and 79-210 $\mu\text{mol m}^{-2} \text{d}^{-1}$ (eastern basin),
392 (both Markaki et al., 2010) and 166 $\mu\text{mol m}^{-2} \text{d}^{-1}$ (Crete) (Theodosi et al., 2019); dust 35 $\text{mg m}^{-2} \text{d}^{-1}$
393 (Crete) (Theodosi et al., 2019) and 3.8-5.3 $\text{mg m}^{-2} \text{d}^{-1}$ (Corsica) (Desboeufs et al., 2018). Our estimate
394 of t-Al (dust) deposition to the Black Sea is also similar to the value reported by Theodosi et al.
395 (2013) based on sampling at two coastal sites ($\sim 6 \text{ mg dust m}^{-2} \text{d}^{-1}$, assuming Al is 8 % of dust by
396 mass). Rainfall rates in the Mediterranean and Black Sea basins during summer are low: 0.72 mm d^{-1}
397 for the western Mediterranean (west of Sicily), 0.36 mm d^{-1} for the eastern Mediterranean, and 1.88
398 mm d^{-1} for the Black Sea (Adler et al., 2003). Dry deposition therefore probably accounts for the
399 majority of total atmospheric fluxes to the basins over the study period, although rainfall
400 composition data over the open Mediterranean are extremely scarce (Desboeufs et al., 2022) so this
401 is difficult to verify.

402 Note that the low EF values observed for some “anthropogenic” elements (e.g. P, V, Ni, Cu and Zn
403 for some samples during Leg 1 in the eastern Mediterranean, and V and Ni during Leg 2; Fig. 5) may
404 imply a higher proportion of the soluble fractions of these elements in coarse aerosols than in other
405 samples encountered during GA04. This, in turn, may suggest that deposition velocities in these
406 cases might be higher than the value (0.1 cm s^{-1}) used in our calculations. Thus, deposition fluxes in
407 these cases may be higher than those given in Table 2, although the absence of aerosol size
408 distribution data for these soluble elements makes the magnitude of such underestimation difficult
409 to quantify.

410

411 Table 2. Mean, median and ranges of dry deposition fluxes for total inorganic nitrogen (TIN),
 412 phosphate (PO₄), mineral dust, soluble Fe (s-Fe), Mn (s-Mn), Ni (s-Ni), Zn (s-Zn) and Cd (s-Cd) over
 413 the western and eastern Mediterranean and Black Sea basins. Note that no data (ND) was collected
 414 for TIN or PO₄ during the Black Sea leg of GA04.

	TIN	PO ₄	dust	s-Fe	s-Mn	s-Ni	s-Zn	s-Cd
	μmol m ⁻² d ⁻¹	nmol m ⁻² d ⁻¹	mg m ⁻² d ⁻¹	nmol m ⁻² d ⁻¹	nmol m ⁻² d ⁻¹	nmol m ⁻² d ⁻¹	nmol m ⁻² d ⁻¹	nmol m ⁻² d ⁻¹
Western Med								
Mean	190	52.7	4.1	347	109	6.10	19.9	0.087
Median	148	47.6	3.4	248	73.3	3.60	12.9	0.080
min	95.1	16.3	0.33	10.9	1.40	0.05	3.98	0.005
max	398	132	12.9	1160	395	44.2	73.0	0.241
Eastern Med								
Mean	164	73.4	21.2	224	140	1.99	32.2	0.099
Median	121	70.1	6.5	122	52.9	1.02	21.0	0.075
min	90.7	17.8	1.7	10.4	0.8	0.03	2.2	0.009
max	382	189	111	1200	1087	9.58	118	0.270
Black Sea								
Mean	ND	ND	8.6	217	198	2.69	23.1	0.086
Median	ND	ND	7.3	156	71	2.87	15.7	0.085
min	ND	ND	3.0	97	25	0.33	6.07	0.019
max	ND	ND	14.2	705	950	6.33	43.3	0.224

415

416 3.7.1 Mediterranean Sea

417 Total inorganic nitrogen and phosphate dry deposition fluxes were of the same order for the
 418 western and eastern Mediterranean basins. However, the ratio of N/P was higher in the western
 419 basin (median = ~3100 and 1700 mol mol⁻¹ in the western and eastern basins, respectively). This is
 420 consistent with the regional gradient in N/P in annual and seasonal atmospheric deposition derived
 421 from modelling studies (Okin et al., 2011; Kanakidou et al., 2020). These N/P ratios suggest that
 422 atmospheric deposition contributes to the phosphate-limited status of the eastern Mediterranean
 423 (Krom et al., 2010; Markaki et al., 2010).

424 Previous observations of atmospheric deposition over an annual cycle have shown total Fe (which
 425 is dominated by mineral dust) flux to be higher in the western than in the eastern Mediterranean
 426 (Guieu et al., 2010b). However, during GA04, the highest (by an order of magnitude) calculated
 427 mineral dust fluxes were in the eastern basin (Table 2). Dust transport to the Mediterranean is highly
 428 seasonal, with peak activity starting in the late spring / early summer in the eastern basin before
 429 migrating into the western basin later in the summer (Moulin et al., 1998; Querol et al., 2009). The
 430 GA04 dust fluxes were broadly consistent with these patterns of dust transport, especially when the
 431 more northerly (and remote from dust sources) route of Leg 3 in the western basin, the short
 432 timescale of the GA04 sampling and the sporadic nature of dust transport events (e.g. Guieu et al.,
 433 2010a; Guieu et al., 2010b) are taken into account.

434 The much higher maximum deposition in the eastern basin observed for dust was not apparent
 435 for the soluble elements (Fe, Mn, Ni, Zn and Cd; Table 2). This was despite the dominance of dust as
 436 a source of Fe and Mn (EFs < 2). Thus the higher fluxes of s-Fe and s-Mn relative to dust in the
 437 western basin probably reflect the prevalence of WEU airmasses encountered there during GA04
 438 and the higher fractional solubility of both elements in this airmass type. The west / east distribution
 439 of s-Ni, Zn and Cd fluxes also appears to be impacted by the air mass regimes encountered during
 440 sampling. All these elements have high fractional solubilities that do not vary strongly between air

441 mass types, so their higher soluble fluxes in the west are due directly to the higher prevalence of
442 polluted air (average EFs in the western basin were at least double those in the east for all these
443 elements). The EF values observed for GA04 are in broad agreement with the results of Guieu et al.
444 (2010b) who estimated that ~ 89% of the Fe deposition flux to the Mediterranean basin was of
445 lithogenic origin, whereas Zn and Cd were predominantly of anthropogenic origin (~ 88 and 96%,
446 respectively).

447 Middag et al. (2022) used a simple water balance model approach combined with water column
448 measurements made during GA04 to suggest that atmospheric inputs of Mn, Ni, Zn and Cd were
449 required to balance the Mediterranean budgets of these elements. Assuming that the aerosol
450 samples collected during GA04 were representative of deposition to the region, mean dry deposition
451 fluxes (Table 2) during summer (June - August) can account for 11 (3.6 – 32) % (Mn), 3.2 (1.1 – 9.6) %
452 (Ni), 8.6 (2.9 – 26) % (Zn) and 1.0 (0.3 – 2.9) % (Cd) of the annual deficit in the surface budgets
453 reported by Middag et al. (2022) in the western Mediterranean and 1.4 (0.5 – 4.3) % of the Ni deficit
454 in the eastern basin (values in parentheses represent the range due to a 3-fold uncertainty in
455 deposition velocity). The values for Ni in the eastern basin may be lower limits, as noted above.
456 Middag et al. did not report a deficit of Mn, Zn or Cd in the eastern Mediterranean.

457 3.7.2 Black Sea

458 Calculated dry deposition fluxes of dust in the Black Sea were similar to those in the western
459 Mediterranean during GA04 (Table 2). Arrivals from North Africa have been reported to account for
460 10% of air mass arrivals over the Black Sea in summer (Kubilay et al., 1995), although similar arrivals
461 were not observed during GA04. However, regions of Europe to the northwest of the Black Sea
462 (which dominated air mass arrivals during Leg 2 of GA04) have previously been reported to be
463 significant sources of crustal elements to the basin (Hacisalihoglu et al., 1992). Modelling studies
464 indicate that the annual average t-Fe (and dust) atmospheric flux to the Black Sea is ~2 orders of
465 magnitude lower than to the Mediterranean (Myriokefalitakis et al., 2018), but the short-term
466 sampling conducted during GA04 do not represent these longer-term trends.

467 Soluble-Fe and Mn dry deposition fluxes to the Black Sea were similar to those to the
468 Mediterranean. As for the western Mediterranean, these elements appeared to have predominantly
469 crustal sources (Fig. 3c & d). However, their relatively high fractional solubility over the Black Sea
470 (Fig. 4 c & d) suggests a higher influence for anthropogenic emissions than observed in the eastern
471 Mediterranean. Unusually for the elements studied here, Ni also followed this pattern of low EF (Fig.
472 5c) and high fractional solubility (Fig. 6c) in the Black Sea. Soluble Zn and Cd dry deposition fluxes in
473 the Black Sea were unequivocally associated with anthropogenic activities (Fig. 5e & f).

474

475 4 Conclusions

476 Aerosol sampling during GA04 has confirmed that trace elements over the Mediterranean and
477 Black seas were influenced by mineral dust and various anthropogenic sources from western and
478 eastern Europe. Although the lithogenic elements (Al, Ti, Mn, Fe, Co, Th) are dominated by crustal
479 sources, their fractional solubilities vary considerably with atmospheric dust load. In most cases,
480 lithogenic element solubilities showed more intense responses to changing dust load than observed
481 in the atmosphere over the Atlantic Ocean, with the GA04 samples having lower solubility in dusty
482 aerosols and often higher solubility in polluted European air masses. The shorter atmospheric
483 transport (and hence lower atmospheric processing and less significant mixing with anthropogenic
484 emissions) of Saharan dust to the Mediterranean than to the Atlantic is probably a major contributor

485 to this behaviour. The distributions of the highly soluble anthropogenic elements (P, V, Ni, Cu, Zn,
486 Cd, Pb) indicated that they had a variety of diverse sources around the European continent, as well
487 as from intense shipping activity in the Mediterranean. Our calculated dry deposition flux values
488 confirm the gradient in the N/P ratio of atmospheric deposition across the Mediterranean basin and
489 that atmospheric deposition can be a significant source of soluble elements (especially Mn and Zn)
490 to the basin.

491 **Data availability:**

492 The data reported in this manuscript have been submitted to the GEOTRACES IDP (soluble
493 element data were submitted to IDP2017, other data is currently being submitted for inclusion in
494 IDP2025) and are also available from the corresponding author on request.

495 **Author contribution:**

496 Writing – original draft preparation: RUS, Writing – review & editing: All authors, Investigation:
497 MT, SM, RUS, Formal analysis: All authors, Conceptualization and Funding acquisition: ARB.

498 **Competing interests:**

499 The authors declare that they have no conflict of interest.

500 **Acknowledgements**

501 We gratefully acknowledge the support and assistance of Micha Rijkenberg, the chief scientist of
502 GA04, Pim Boute (Leg 1), Morten Andersen (Leg 2), Eyal Wurgaft and Simona Brogi (Leg 3) for
503 sampling, and the captain and crew of RV *Pelagia* during the voyage. This work was funded by the
504 Dutch Research Council (project number 822.01.015), the UK Natural Environment Research Council
505 (grant number NE/V001213/1) and the University of East Anglia. The International GEOTRACES
506 Programme is possible in part thanks to the support from the U.S. National Science Foundation
507 (OCE-2140395) to the Scientific Committee on Oceanic Research (SCOR). Global Precipitation
508 Climatology Project (GPCP) Monthly Analysis Product data was provided by the NOAA PSL, Boulder,
509 Colorado, USA, from their website at <https://psl.noaa.gov>. We thank Karine Desboeufs and two
510 anonymous reviewers for their helpful comments.

511 **References**

512

- 513 Adler, R. F., Huffman, G. J., Chang, A., Ferraro, R., Xie, P., Janowiak, J., Rudolf, B., Schneider, U.,
514 Curtis, S., Bolvin, D., Gruber, A., Susskind, J., and Arkin, P. A.: The Version 2 Global Precipitation
515 Climatology Project (GPCP) Monthly Precipitation Analysis (1979-Present), *Journal of*
516 *Hydrometeorology*, 4, 1147-1167, 2003.
- 517 Baker, A. R., Jickells, T. D., Witt, M., and Linge, K. L.: Trends in the solubility of iron, aluminium,
518 manganese and phosphorus in aerosol collected over the Atlantic Ocean, *Marine Chemistry*, 98, 43-
519 58, 10.1016/j.marchem.2005.06.004, 2006.
- 520 Baker, A. R., Weston, K., Kelly, S. D., Voss, M., Streu, P., and Cape, J. N.: Dry and wet deposition of
521 nutrients from the tropical Atlantic atmosphere: links to primary productivity and nitrogen fixation,
522 *Deep-Sea Research Part I*, 54, 1704-1720, 10.1016/j.dsr.2007.07.001, 2007.
- 523 Baker, A. R., and Croot, P. L.: Atmospheric and marine controls on aerosol iron solubility in seawater,
524 *Marine Chemistry*, 120, 4-13, 10.1016/j.marchem.2008.09.003, 2010.
- 525 Baker, A. R., and Jickells, T. D.: Atmospheric deposition of soluble trace elements along the Atlantic
526 Meridional Transect (AMT), *Progress in Oceanography*, 158, 41-51, 10.1016/j.pocean.2016.10.002,
527 2017.

528 Baker, A. R., Li, M., and Chance, R. J.: Trace metal fractional solubility in size-segregated aerosols
529 from the tropical eastern Atlantic Ocean, *Global Biogeochemical Cycles*, 34, e2019GB006510,
530 10.1029/2019GB006510, 2020.

531 Baker, A. R., Kanakidou, M., Nenes, A., Myriokefalitakis, S., Croot, P. L., Duce, R. A., Gao, Y., Ito, A.,
532 Jickells, T. D., Mahowald, N. M., Middag, R., Perron, M. M. G., Sarin, M. M., Shelley, R. U., and
533 Turner, D. R.: Changing atmospheric acidity as a modulator of nutrient deposition and ocean
534 biogeochemistry, *Science Advances*, 7, eabd8800, 10.1126/sciadv.abd8800, 2021.

535 Becagli, S., Sferlazzo, D. M., Pace, G., di Sarra, A., Bommarito, C., Calzolari, G., Ghedini, C., Lucarelli, F.,
536 Meloni, D., Monteleone, F., Severi, M., Traversi, R., and Udisti, R.: Evidence for heavy fuel oil
537 combustion aerosols from chemical analyses at the island of Lampedusa: a possible large role of
538 ships emissions in the Mediterranean, *Atmospheric Chemistry and Physics*, 12, 3479-3492,
539 10.5194/acp-12-3479-2012, 2012.

540 Boyle, E. A., Chapnick, S. D., Bai, X. X., and Spivack, A.: Trace metal enrichments in the
541 Mediterranean Sea, *Earth and Planetary Science Letters*, 74, 405-419, 10.1016/s0012-
542 821x(85)80011-x, 1985.

543 Bridgestock, L., van de Flierdt, T., Rehkämper, M., Paul, M., Middag, R., Milne, A., Lohan, M. C.,
544 Baker, A. R., Chance, R., Khondoker, R., Strekopytov, S., Humphreys-Williams, E., Achterberg, E. P.,
545 Rijkenberg, M. J. A., Gerringa, L. J. A., and De Baar, H. J. W.: Return of naturally sourced Pb to
546 Atlantic surface waters, *Nature Communications*, 7, 12921, 10.1038/ncomms12921, 2016.

547 Buck, C. S., Landing, W. M., Resing, J. A., and Measures, C. I.: The solubility and deposition of aerosol
548 Fe and other trace elements in the North Atlantic Ocean: Observations from the A16N CLIVAR/CO₂
549 repeat hydrography section, *Marine Chemistry*, 210, 57-70, 10.1016/j.marchem.2008.08.003, 2010.

550 Carslaw, K. S., Boucher, O., Spracklen, D. V., Mann, G. W., Rae, J. G. L., Woodward, S., and Kulmala,
551 M.: A review of natural aerosol interactions and feedbacks within the Earth system, *Atmospheric
552 Chemistry and Physics*, 10, 1701-1737, 10.5194/acp-10-1701-2010, 2010.

553 Chance, R., Jickells, T. D., and Baker, A. R.: Atmospheric trace metal concentrations, solubility and
554 deposition fluxes in remote marine air over the south-east Atlantic, *Marine Chemistry*, 177, 45-56,
555 10.1016/j.marchem.2015.06.028, 2015.

556 Chester, R., Saydam, A. C., and Sharples, E. J.: An approach to the assessment of local trace-metal
557 pollution in the Mediterranean marine atmosphere, *Marine Pollution Bulletin*, 12, 426-431,
558 10.1016/0025-326x(81)90161-2, 1981.

559 Chester, R., Sharples, E. J., Sanders, G. S., and Saydam, A. C.: Saharan dust incursion over the
560 Tyrrhenian Sea, *Atmospheric Environment (1967)*, 18, 929-935, 10.1016/0004-6981(84)90069-6,
561 1984.

562 Chester, R., Nimmo, M., Alarcon, M., Saydam, C., Murphy, K. J. T., Sanders, G. S., and Corcoran, P.:
563 Defining the chemical character of aerosols from the atmosphere of the Mediterranean Sea and
564 surrounding regions, *Oceanol. Acta*, 16, 231-246, 1993.

565 Chiapello, I., Bergametti, G., Chatenet, B., Bousquet, P., Dulac, F., and Santos Soares, E.: Origins of
566 African dust transported over the northeastern tropical Atlantic, *Journal of Geophysical Research*,
567 102, 13701-13709, 10.1029/97JD00259, 1997.

568 de Leeuw, G., Andreas, E. L., Anguelova, M. D., Fairall, C. W., Lewis, E. R., O'Dowd, C., Schulz, M., and
569 Schwartz, S. E.: Production flux of sea spray aerosol, *Reviews of Geophysics*, 49, RG2001,
570 [10.1029/2010RG000349](https://doi.org/10.1029/2010RG000349), 2011.

571 Desboeufs, K., Nguyen, E. B., Chevaillier, S., Triquet, S., and Dulac, F.: Fluxes and sources of nutrient
572 and trace metal atmospheric deposition in the northwestern Mediterranean, *Atmospheric Chemistry
573 and Physics*, 18, 14477-14492, 10.5194/acp-18-14477-2018, 2018.

574 Desboeufs, K., Fu, F., Bressac, M., Tovar-Sanchez, A., Triquet, S., Doussin, J. F., Giorio, C., Chazette,
575 P., Disnaquet, J., Feron, A., Formenti, P., Maisonneuve, F., Rodriguez-Romero, A., Zapf, P., Dulac, F.,
576 and Guieu, C.: Wet deposition in the remote western and central Mediterranean as a source of trace
577 metals to surface seawater, *Atmospheric Chemistry and Physics*, 22, 2309-2332, 10.5194/acp-22-
578 2309-2022, 2022.

579 Desboeufs, K. V., Sofikitis, A., Losno, R., Colin, J. L., and Ausset, P.: Dissolution and solubility of trace
580 metals from natural and anthropogenic aerosol particulate matter, *Chemosphere*, 58, 195-203,
581 10.1016/j.chemosphere.2004.02.025, 2005.

582 Duce, R. A., Liss, P. S., Merrill, J. T., Atlas, E. L., Buat-Menard, P., Hicks, B. B., Miller, J. M., Prospero, J.
583 M., Arimoto, R., Church, T. M., Ellis, W., Galloway, J. N., Hansen, L., Jickells, T. D., Knap, A. H.,
584 Reinhardt, K. H., Schneider, B., Soudine, A., Tokos, J. J., Tsunogai, S., Wollast, R., and Zhou, M.: The
585 atmospheric input of trace species to the world ocean, *Global Biogeochemical Cycles*, 5, 193-259,
586 10.1029/91GB01778, 1991.

587 Dulaquais, G., Planquette, H., L'Helguen, S., Rijkenberg, M. J. A., and Boye, M.: The biogeochemistry
588 of cobalt in the Mediterranean Sea, *Global Biogeochemical Cycles*, 31, 377-399,
589 10.1002/2016gb0054780, 2017.

590 Fang, T., Guo, H., Zeng, L., Verma, V., Nenes, A., and Weber, R. J.: Highly acidic ambient particles,
591 soluble metals, and oxidative potential: A link between sulfate and aerosol toxicity, *Environmental
592 Science & Technology*, 51, 2611-2620, 10.1021/acs.est.6b06151, 2017.

593 Gerringa, L. J. A., Slagter, H. A., Bown, J., van Haren, H., Laan, P., de Baar, H. J. W., and Rijkenberg, M.
594 J. A.: Dissolved Fe and Fe-binding organic ligands in the Mediterranean Sea GEOTRACES G04, *Marine
595 Chemistry*, 194, 100-113, 10.1016/j.marchem.2017.05.012, 2017.

596 Gkikas, A., Hatzianastassiou, N., Mihalopoulos, N., Katsoulis, V., Kazadzis, S., Pey, J., Querol, X., and
597 Torres, O.: The regime of intense desert dust episodes in the Mediterranean based on contemporary
598 satellite observations and ground measurements, *Atmospheric Chemistry and Physics*, 13, 12135-
599 12154, 10.5194/acp-13-12135-2013, 2013.

600 Guieu, C., Martin, J. M., Tankere, S. P. C., Mousty, F., Trincherini, P., Bazot, M., and Dai, M. H.: On
601 trace metal geochemistry in the Danube River and western Black Sea, *Estuarine Coastal and Shelf
602 Science*, 47, 471-485, 10.1006/ecss.1998.0377, 1998.

603 Guieu, C., Dulac, F., Desboeufs, K., Wagener, T., Pulido-Villena, E., Grisoni, J. M., Louis, F., Ridame, C.,
604 Blain, S., Brunet, C., Nguyen, E. B., Tran, S., Labiadh, M., and Dominici, J. M.: Large clean mesocosms
605 and simulated dust deposition: a new methodology to investigate responses of marine oligotrophic
606 ecosystems to atmospheric inputs, *Biogeosciences*, 7, 2765-2784, 10.5194/bg-7-2765-2010, 2010a.

607 Guieu, C., Loÿe-Pilot, M.-D., Benyahya, L., and Dufour, A.: Spatial variability of atmospheric fluxes of
608 metals (Al, Fe, Cd, Zn and Pb) and phosphorus over the whole Mediterranean from a one-year
609 monitoring experiment: Biogeochemical implications, *Marine Chemistry*, 120, 164-178, 2010b.

610 Guinoiseau, D., Singh, S. P., Galer, S. J. G., Abouchami, W., Bhattacharyya, R., Kandler, K., Bristow, C.,
611 and Andreae, M. O.: Characterization of Saharan and Sahelian dust sources based on geochemical
612 and radiogenic isotope signatures, *Quaternary Science Reviews*, 293, 107729,
613 10.1016/j.quascirev.2022.107729, 2022.

614 Hacısalihoglu, G., Eliyakut, F., Olmez, I., Balkas, T. I., and Tuncel, G.: Chemical composition of
615 particles in the Black Sea atmosphere, *Atmospheric Environment Part A-General Topics*, 26, 3207-
616 3218, 10.1016/0960-1686(92)90477-3, 1992.

617 Hamilton, D. S., Perron, M. M. G., Bond, T. C., Bowie, A. R., Buchholz, R. R., Guieu, C., Ito, A.,
618 Maenhaut, W., Myriokefalitakis, S., Olgun, N., Rathod, S. D., Schepanski, K., Tagliabue, A., Wagner,
619 R., and Mahowald, N. M.: Earth, Wind, Fire, and Pollution: Aerosol nutrient sources and impacts on
620 ocean biogeochemistry, *Annual Review of Marine Science*, 14, 303-330, 10.1146/annurev-marine-
621 031921-013612, 2022.

622 Heimbürger, L. E., Migon, C., Dufour, A., Chiffolleau, J. F., and Cossa, D.: Trace metal concentrations
623 in the North-western Mediterranean atmospheric aerosol between 1986 and 2008: Seasonal
624 patterns and decadal trends, *Science of the Total Environment*, 408, 2629-2638,
625 10.1016/j.scitotenv.2010.02.042, 2010.

626 Hernandez, C., Drobinski, P., and Turquety, S.: How much does weather control fire size and intensity
627 in the Mediterranean region?, *Annales Geophysicae*, 33, 931-939, 10.5194/angeo-33-931-2015,
628 2015.

629 Herut, B., Nimmo, M., Medway, A., Chester, R., and Krom, M. D.: Dry atmospheric inputs of trace
630 metals at the Mediterranean coast of Israel (SE Mediterranean): sources and fluxes, *Atmospheric*
631 *Environment*, 35, 803-813, 10.1016/s1352-2310(00)00216-8, 2001.

632 Herut, B., Rahav, E., Tsagaraki, T. M., Giannakourou, A., Tsiola, A., Psarra, S., Lagaria, A.,
633 Papageorgiou, N., Mihalopoulos, N., Theodosi, C. N., Violaki, K., Stathopoulou, E., Scoullou, M., Krom,
634 M. D., Stockdale, A., Shi, Z., Berman-Frank, I., Meador, T. B., Tanaka, T., and Paraskevi, P.: The
635 potential impact of Saharan dust and polluted aerosols on microbial populations in the East
636 Mediterranean Sea, an overview of a mesocosm experimental approach, *Frontiers in Marine*
637 *Science*, 3, 226, 10.3389/fmars.2016.00226, 2016.

638 Hsu, S. C., Lin, F. J., and Jeng, W. L.: Seawater solubility of natural and anthropogenic metals within
639 ambient aerosols collected from Taiwan coastal sites, *Atmospheric Environment*, 39, 3989-4001,
640 10.1016/j.atmosenv.2005.03.033, 2005.

641 Jickells, T., and Moore, C. M.: The importance of atmospheric deposition for ocean productivity, in:
642 *Annual Review of Ecology, Evolution, and Systematics*, Vol 46, edited by: Futuyma, D. J., *Annual*
643 *Review of Ecology Evolution and Systematics*, 481-501, 2015.

644 Jickells, T. D., An, Z. S., Anderson, K. K., Baker, A. R., Bergametti, G., Brooks, N., Cao, J. J., Boyd, P. W.,
645 Duce, R. A., Hunter, K. A., Kawahata, H., Kubilay, N., La Roche, J., Liss, P. S., Mahowald, N., Prospero,
646 J. M., Ridgwell, A. J., Tegen, I., and Torres, R.: Global Iron Connections between desert dust, ocean
647 biogeochemistry and climate, *Science*, 308, 67-71, 2005.

648 Jickells, T. D., Baker, A. R., and Chance, R.: Atmospheric transport of trace elements and nutrients to
649 the oceans, *Philosophical Transactions of the Royal Society of London Series A-Mathematical*
650 *Physical and Engineering Sciences*, 374, 20150286, 10.1098/rsta.2015.0286, 2016.

651 Kanakidou, M., Myriokefalitakis, S., and Tsagkaraki, M.: Atmospheric inputs of nutrients to the
652 Mediterranean Sea, *Deep Sea Research Part II: Topical Studies in Oceanography*, 171, 104606,
653 10.1016/j.dsr2.2019.06.014, 2020.

654 Kandler, K., Benker, N., Bundke, U., Cuevas, E., Ebert, M., Knippertz, P., Rodriguez, S., Schütz, L., and
655 Weinbruch, S.: Chemical composition and complex refractive index of Saharan Mineral Dust at Izana,
656 Tenerife (Spain) derived by electron microscopy, *Atmospheric Environment*, 41, 8058-8074,
657 10.1016/j.atmosenv.2007.06.047, 2007.

658 Koçak, M., Mihalopoulos, N., and Kubilay, N.: Contributions of natural sources to high PM₁₀ and
659 PM_{2.5} events in the eastern Mediterranean, *Atmospheric Environment*, 41, 3806-3818,
660 10.1016/j.atmosenv.2007.01.009, 2007.

661 Krom, M. D., Emeis, K. C., and Van Cappellen, P.: Why is the Eastern Mediterranean phosphorus
662 limited?, *Progress in Oceanography*, 85, 236-244, 10.1016/j.pocean.2010.03.003, 2010.

663 Kubilay, N., and Saydam, A. C.: Trace elements in atmospheric particulates over the eastern
664 Mediterranean - concentrations, sources, and temporal variability, *Atmospheric Environment*, 29,
665 2289-2300, 10.1016/1352-2310(95)00101-4, 1995.

666 Kubilay, N., Yemencioğlu, S., and Saydam, A. C.: Airborne material collections and their chemical
667 composition over the Black Sea, *Marine Pollution Bulletin*, 30, 475-483, 10.1016/0025-
668 326x(95)00238-i, 1995.

669 Kumar, A., and Sarin, M. M.: Aerosol iron solubility in a semi-arid region: temporal trend and impact
670 of anthropogenic sources, *Tellus*, 62B, 125-132, 10.1111/j.1600-0889.2009.00448.x, 2010.

671 Lelieveld, J., Berresheim, H., Borrmann, S., Crutzen, P. J., Dentener, F. J., Fischer, H., Feichter, J.,
672 Flatau, P. J., Heland, J., Holzinger, R., Korrmann, R., Lawrence, M. G., Levin, Z., Markowicz, K. M.,
673 Mihalopoulos, N., Minikin, A., Ramanathan, V., de Reus, M., Roelofs, G. J., Scheeren, H. A., Sciare, J.,
674 Schlager, H., Schultz, M., Siegmund, P., Steil, B., Stephanou, E. G., Stier, P., Traub, M., Warneke, C.,
675 Williams, J., and Ziereis, H.: Global air pollution crossroads over the Mediterranean, *Science*, 298,
676 794-799, 10.1126/science.1075457, 2002.

677 Li, R., Zhang, H. H., Wang, F., Ren, Y., Jia, S. G., Jiang, B., Jia, X. H., Tang, Y. J., and Tang, M. J.:
678 Abundance and fractional solubility of phosphorus and trace metals in combustion ash and desert

679 dust: Implications for bioavailability and reactivity, *Science of the Total Environment*, 816, 151495,
680 10.1016/j.scitotenv.2021.151495, 2022.

681 Longo, A. F., Feng, Y., Lai, B., Landing, W. M., Shelley, R. U., Nenes, A., Mihalopoulos, N., Violaki, K.,
682 and Ingall, E. D.: Influence of atmospheric processes on the solubility and composition of iron in
683 Saharan dust, *Environmental Science & Technology*, 50, 6912-6920, 10.1021/acs.est.6b02605, 2016.

684 Mahowald, N., Jickells, T. D., Baker, A. R., Artaxo, P., Benitez-Nelson, C. R., Bergametti, G., Bond, T.
685 C., Chen, Y., Cohen, D. D., Herut, B., Kubilay, N., Losno, R., Luo, C., Maenhaut, W., McGee, K. A., Okin,
686 G. S., Siefert, R. L., and Tsukuda, S.: The global distribution of atmospheric phosphorus sources,
687 concentrations and deposition rates, and anthropogenic impacts, *Global Biogeochemical Cycles*, 22,
688 GB4026, 10.1029/2008GB003240, 2008.

689 Markaki, Z., Loye-Pilot, M. D., Violaki, K., Benyahya, L., and Mihalopoulos, N.: Variability of
690 atmospheric deposition of dissolved nitrogen and phosphorus in the Mediterranean and possible
691 link to the anomalous seawater N/P ratio, *Marine Chemistry*, 120, 187-194, 2010.

692 Martin, J. H.: Glacial-Interglacial CO₂ change: the iron hypothesis, *Paleoceanography*, 5, 1-13, 1990.

693 Middag, R., Rolison, J. M., George, E., Gerringa, L. J. A., Rijkenberg, M. J. A., and Stirling, C. H.: Basin
694 scale distributions of dissolved manganese, nickel, zinc and cadmium in the Mediterranean Sea,
695 *Marine Chemistry*, 238, 104063, 10.1016/j.marchem.2021.104063, 2022.

696 Moreno, T., Perez, N., Querol, X., Amato, F., Alastuey, A., Bhatia, R., Spiro, B., Hanvey, M., and
697 Gibbons, W.: Physicochemical variations in atmospheric aerosols recorded at sea onboard the
698 Atlantic-Mediterranean 2008 Scholar Ship cruise (Part II): Natural versus anthropogenic influences
699 revealed by PM₁₀ trace element geochemistry, *Atmospheric Environment*, 44, 2563-2576,
700 10.1016/j.atmosenv.2010.04.027, 2010.

701 Moulin, C., Lambert, C. E., Dayan, U., Masson, V., Ramonet, M., Bousquet, P., Legrand, M., Balkanski,
702 Y. J., Guelle, W., Marticorena, B., Bergametti, G., and Dulac, F.: Satellite climatology of African dust
703 transport in the Mediterranean atmosphere, *Journal of Geophysical Research: Atmospheres*, 103,
704 13137-13144, 10.1029/98JD00171, 1998.

705 Myriokefalitakis, S., Ito, A., Kanakidou, M., Nenes, A., Krol, M. C., Mahowald, N. M., Scanza, R. A.,
706 Hamilton, D. S., Johnson, M. S., Meskhidze, N., Kok, J. F., Guieu, C., Baker, A. R., Jickells, T. D., Sarin,
707 M. M., Bikkina, S., Shelley, R. U., Bowie, A., Perron, M. M. G., and Duce, R. A.: The GESAMP
708 atmospheric iron deposition model intercomparison study, *Biogeosciences*, 15, 6659-6684,
709 10.5194/bg-15-6659-2018, 2018.

710 Okin, G., Baker, A. R., Tegen, I., Mahowald, N. M., Dentener, F. J., Duce, R. A., Galloway, J. N., Hunter,
711 K., Kanakidou, M., Kubilay, N., Prospero, J. M., Sarin, M., Surapipith, V., Uematsu, M., and Zhu, T.:
712 Impacts of atmospheric nutrient deposition on marine productivity: roles of nitrogen, phosphorus,
713 and iron, *Global Biogeochemical Cycles*, 25, GB2022, 10.1029/2010GB003858, 2011.

714 Pacyna, J. M., and Pacyna, E. G.: An assessment of global and regional emissions of trace metals to
715 the atmosphere from anthropogenic sources worldwide, *Environmental Reviews*, 9, 269-298,
716 10.1139/a01-012, 2001.

717 Pye, H. O. T., Nenes, A., Alexander, B., Ault, A. P., Barth, M. C., Clegg, S. L., Collett Jr, J. L., Fahey, K.
718 M., Hennigan, C. J., Herrmann, H., Kanakidou, M., Kelly, J. T., Ku, I. T., McNeill, V. F., Riemer, N.,
719 Schaefer, T., Shi, G., Tilgner, A., Walker, J. T., Wang, T., Weber, R., Xing, J., Zaveri, R. A., and Zuend,
720 A.: The acidity of atmospheric particles and clouds, *Atmospheric Chemistry and Physics*, 20, 4809-
721 4888, 10.5194/acp-2019-889, 2020.

722 Querol, X., Pey, J., Pandolfi, M., Alastuey, A., Cusack, M., Pérez, N., Moreno, T., Viana, M.,
723 Mihalopoulos, N., Kallos, G., and Kleanthous, S.: African dust contributions to mean ambient PM₁₀
724 mass-levels across the Mediterranean Basin, *Atmospheric Environment*, 43, 4266-4277,
725 10.1016/j.atmosenv.2009.06.013, 2009.

726 Rolison, J. M., Middag, R., Stirling, C. H., Rijkenberg, M. J. A., and de Baar, H. J. W.: Zonal distribution
727 of dissolved aluminium in the Mediterranean Sea, *Marine Chemistry*, 177, 87-100,
728 10.1016/j.marchem.2015.05.001, 2015.

729 Scerri, M. M., Kandler, K., and Weinbruch, S.: Disentangling the contribution of Saharan dust and
730 marine aerosol to PM₁₀ levels in the Central Mediterranean, *Atmospheric Environment*, 147, 395-
731 408, 10.1016/j.atmosenv.2016.10.028, 2016.

732 Shelley, R. U., Morton, P. L., and Landing, W. M.: Elemental ratios and enrichment factors in aerosols
733 from the US-GEOTRACES North Atlantic transects, *Deep Sea Research Part II: Topical Studies in*
734 *Oceanography*, 116, 262-272, 10.1016/j.dsr2.2014.12.005, 2015.

735 Shelley, R. U., Roca-Marti, M., Castrillejo, M., Masque, P., Landing, W. M., Planquette, H., and
736 Sarthou, G.: Quantification of trace element atmospheric deposition fluxes to the Atlantic Ocean (>
737 40°N; GEOVIDE, GEOTRACES GA01) during spring 2014, *Deep-Sea Research Part I-Oceanographic*
738 *Research Papers*, 119, 34-49, 10.1016/j.dsr.2016.11.010, 2017.

739 Shelley, R. U., Landing, W. M., Ussher, S. J., Planquette, H., and Sarthou, G.: Regional trends in the
740 fractional solubility of Fe and other metals from North Atlantic aerosols (GEOTRACES cruises GA01
741 and GA03) following a two-stage leach, *Biogeosciences*, 15, 2271-2288, 10.5194/bg-15-2271-2018,
742 2018.

743 Shi, Z., Krom, M. D., Bonneville, S., Baker, A. R., Bristow, C., Drake, N., Mann, G., Carslaw, K.,
744 McQuaid, J. B., Jickells, T., and Benning, L. G.: Influence of chemical weathering and aging of iron
745 oxides on the potential iron solubility of Saharan dust during simulated atmospheric processing,
746 *Global Biogeochemical Cycles*, 25, GB2010, 10.1029/2010GB003837, 2011.

747 Sholkovitz, E. R., Sedwick, P. N., and Church, T. M.: Influence of anthropogenic combustion emissions
748 on the deposition of soluble aerosol iron to the ocean: Empirical estimates for island sites in the
749 North Atlantic, *Geochimica et Cosmochimica Acta*, 73, 3981-4003, 2009.

750 Sholkovitz, E. R., Sedwick, P. N., Church, T. M., Baker, A. R., and Powell, C. F.: Fractional solubility of
751 aerosol iron: Synthesis of a global-scale data set, *Geochimica et Cosmochimica Acta*, 89, 173-189,
752 10.1016/j.gca.2012.04.022 2012.

753 Spokes, L. J., and Jickells, T. D.: Factors controlling the solubility of aerosol trace metals in the
754 atmosphere and on mixing into seawater, *Aquatic Geochemistry*, 1, 355-374, 1996.

755 Stein, A. F., Draxler, R. R., Rolph, G. D., Stunder, B. J. B., Cohen, M. D., and Ngan, F.: NOAA's HYSPLIT
756 atmospheric transport and dispersion modeling system, *Bulletin of the American Meteorological*
757 *Society*, 96, 2059-2077, 10.1175/bams-d-14-00110.1, 2015.

758 Theodosi, C., Markaki, Z., and Mihalopoulos, N.: Iron speciation, solubility and temporal variability in
759 wet and dry deposition in the Eastern Mediterranean, *Marine Chemistry*, 120, 100-107, 2010a.

760 Theodosi, C., Markaki, Z., Tselepidis, A., and Mihalopoulos, N.: The significance of atmospheric
761 inputs of soluble and particulate major and trace metals to the eastern Mediterranean seawater,
762 *Marine Chemistry*, 120, 154-163, 10.1016/j.marchem.2010.02.003, 2010b.

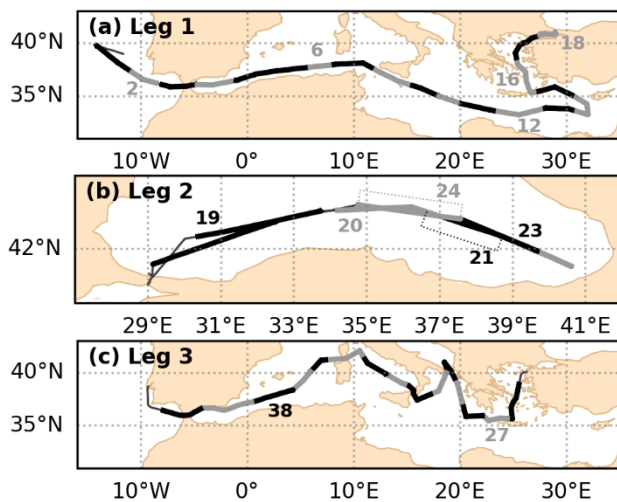
763 Theodosi, C., Stavrakakis, S., Koulaki, F., Stavrakaki, I., Moncheva, S., Papathanasiou, E., Sanchez-
764 Vidal, A., Koçak, M., and Mihalopoulos, N.: The significance of atmospheric inputs of major and trace
765 metals to the Black Sea, *Journal of Marine Systems*, 109-110, 94-102,
766 10.1016/j.jmarsys.2012.02.016, 2013.

767 Theodosi, C., Markaki, Z., Pantazoglou, F., Tselepidis, A., and Mihalopoulos, N.: Chemical
768 composition of downward fluxes in the Cretan Sea (Eastern Mediterranean) and possible link to
769 atmospheric deposition: A 7 year survey, *Deep-Sea Research Part II-Topical Studies in Oceanography*,
770 164, 89-99, 10.1016/j.dsr2.2019.06.003, 2019.

771 Tovar-Sanchez, A., Duarte, C. M., Arrieta, J. M., and Sanudo-Wilhelmy, S.: Spatial gradients in trace
772 metal concentrations in the surface microlayer of the Mediterranean Sea, *Frontiers in Marine*
773 *Science*, 1, 79, 10.3389/fmars.2014.00079, 2014.

774 Turekian, K. K., and Wedepohl, K. H.: Distribution of the elements in some major units of the Earth's
775 crust, *Geological Society of America Journal*, 72, 175-191, 1961.

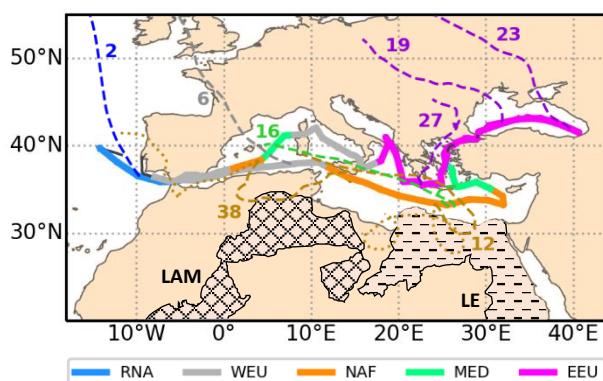
776 Westberry, T. K., Behrenfeld, M. J., Shi, Y. R., Yu, H., Remer, L. A., and Bian, H.: Atmospheric
777 nourishment of global ocean ecosystems, *Science*, 380, 515-519, 10.1126/science.abq5252, 2023.



780

781 [Figure 1. GA04 cruise track showing aerosol sampling periods as alternating thick black and grey bars](#)
 782 [for \(a\) Leg 1, \(b\) Leg 2 and \(c\) Leg 3. Note that the eastbound and westbound sections of Leg 2](#)
 783 [followed very similar tracks and cannot be distinguished on this map. Numbers for samples referred](#)
 784 [to in the text and in Fig. 2 are indicated.](#)

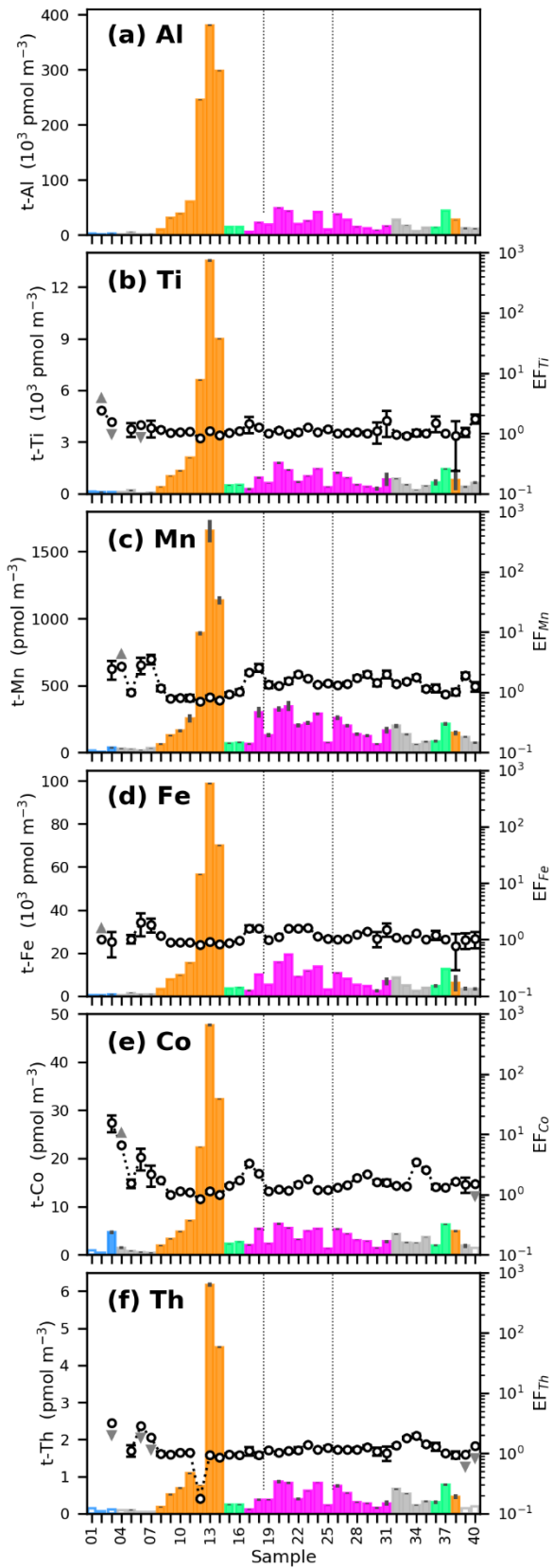
785



786

787 [Figure 2. GA04 cruise track showing the classification of aerosol samples into 5 air mass types.](#)
 788 [Example AMBTs \(and sample numbers\) for each type are shown for arrivals at 10 m \(dashed lines\)](#)
 789 [and \(for NAF only\) 1000 m \(dotted lines\). The Libya-Algeria-Mali \(LAM\) and Libya-Egypt \(LE\) Potential](#)
 790 [Source Areas \(Guinoiseau et al., 2022\) are also shown.](#)

791



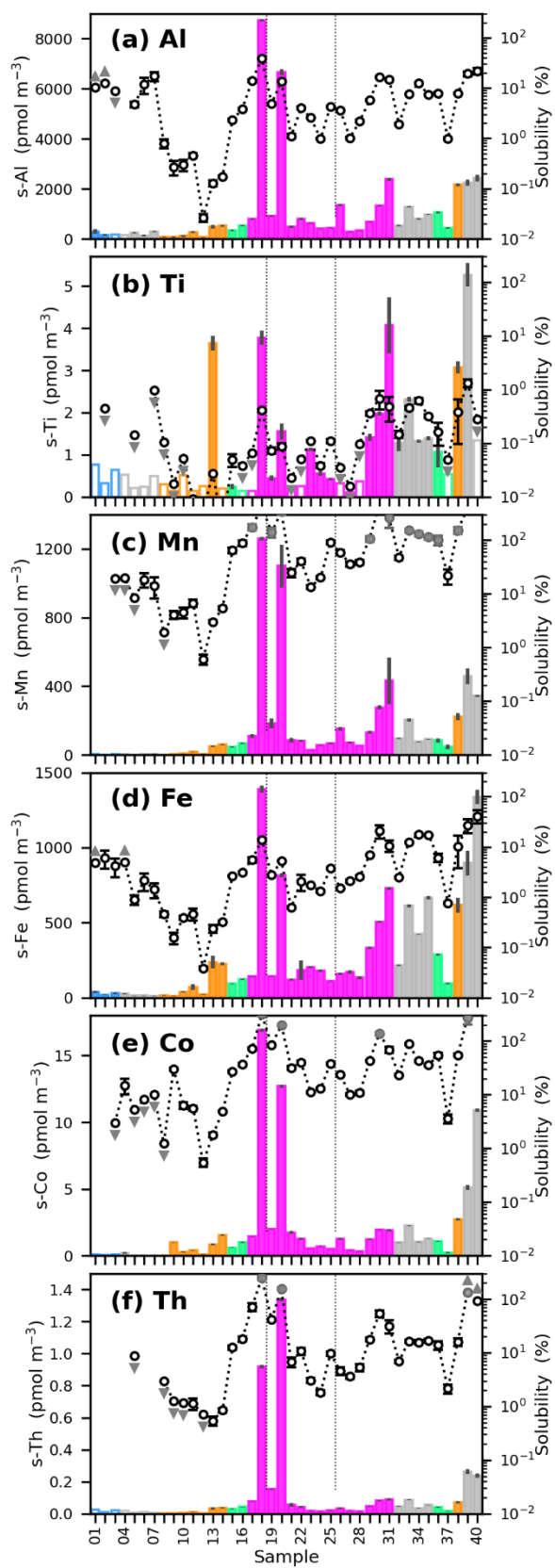
792

793

794

Figure 3. Total concentrations of lithogenic elements $\pm 1 \text{ SD}$ (pmol m^{-3}), with enrichment factors relative to Al overlaid (circles). Unfilled bars indicate that analyte was below the limit of detection

795 and bar represents 75% of the limit of detection. An EF was not determined if both AI and the
796 element of interest were below the limit of detection. Up- / down-ward pointing grey arrows near EF
797 markers indicate that values are minima / maxima because AI / the element were below the limit of
798 detection. Bars are coloured according to the air mass type of each sample, blue = RNA, grey = WEU,
799 orange = NAF, green = MED, pink = EEU. The dashed grey vertical lines indicate the legs of the cruise,
800 with Leg 1-3 being left to right.

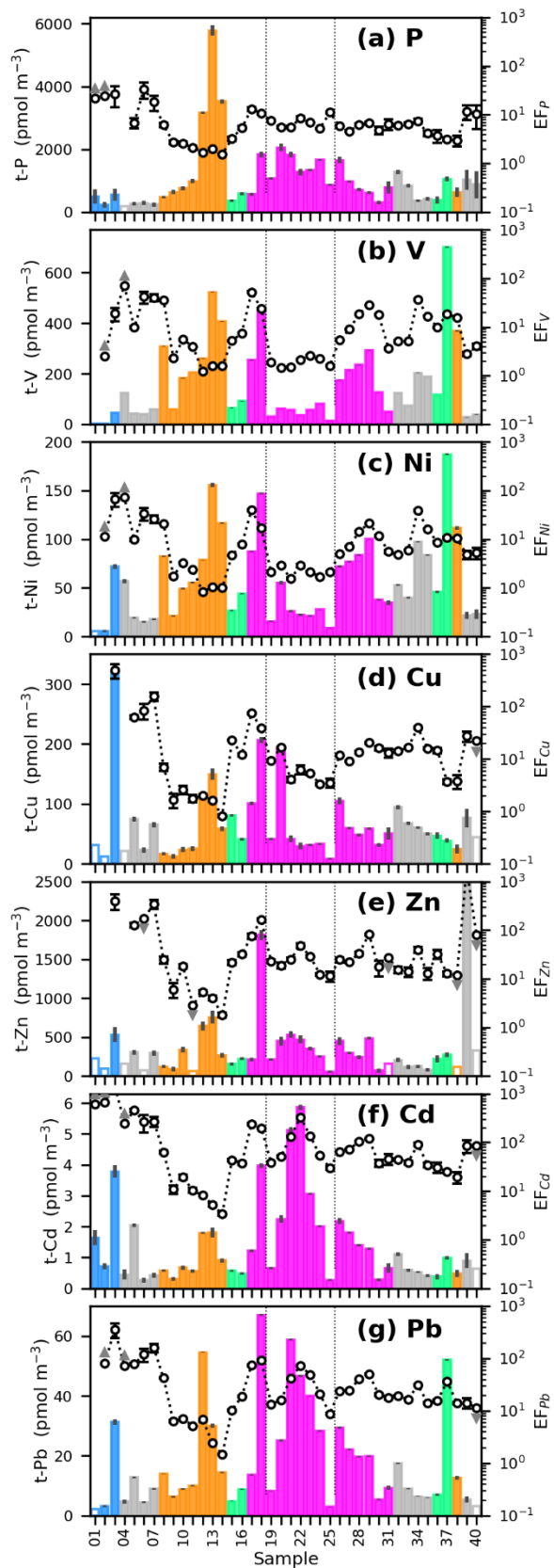


801

802 [Figure 4. Soluble concentrations of lithogenic metals \$\pm 1\$ SD \(\$\text{pmol m}^{-3}\$ \), with fractional solubility](#)
 803 [overlaid \(circles\). Up- / down-ward pointing grey arrows near solubility markers indicate that values](#)

804 [are minima / maxima because total / soluble concentrations were below the limit of detection. Note](#)
805 [that the axis for fractional solubility is capped at 300%. This is because there were a few instances of](#)
806 [solubility >100% \(grey circles\), suggesting some low-level contamination of those samples. Rather](#)
807 [than set these solubilities to a maximum of 100%, we chose this approach to make it clear which](#)
808 [samples this applied to. Bar colours and dashed vertical lines are described in Fig. 3.](#)

809

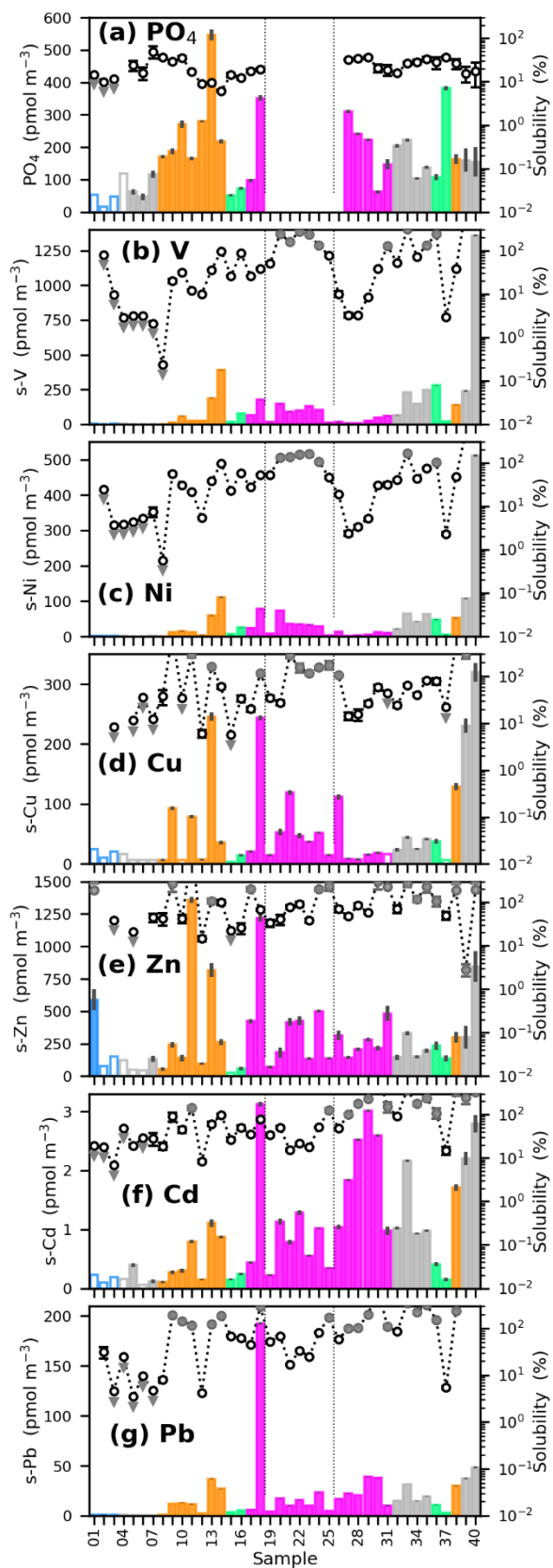


810

811 [Figure 5. Total concentrations of anthropogenic elements \$\pm 1\$ SD \(\$\text{pmol m}^{-3}\$ \), with enrichment factors](#)
 812 [overlaid. Note that Zn contamination of sample TM39 \(\$10500 \text{ pmol m}^{-3}\$ \) is strongly suspected so the](#)

813 y-axis for the Zn data is limited to 2500 pmol m⁻³. Similarly, the EF_{Zn} axis is limited to 1000 as the
814 calculation for EF_{Zn} for TM39 was made using the suspect data point. Bar colours, grey arrows and
815 dashed vertical lines are described in Fig. 3.

816

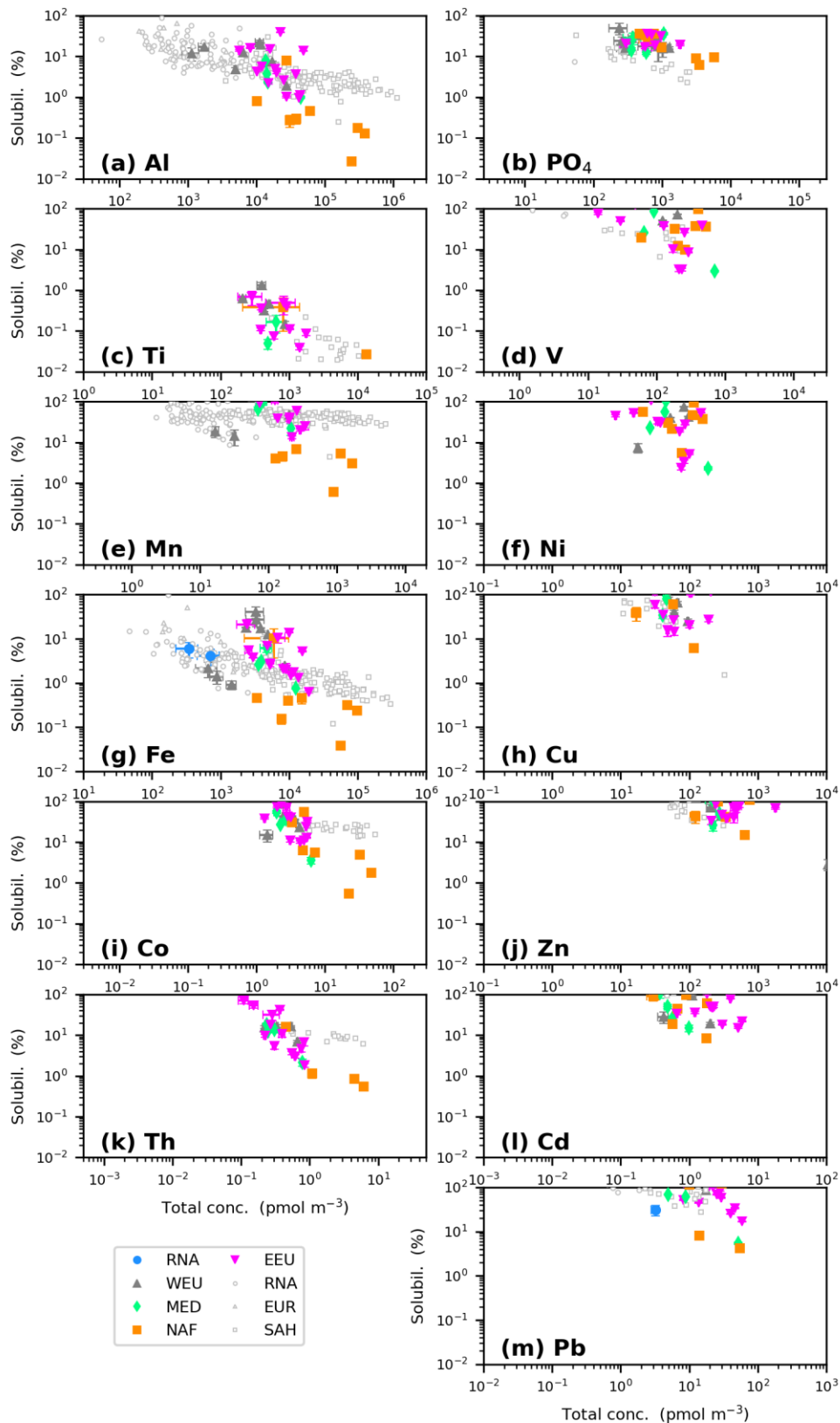


817

818 [Figure 6. Soluble concentrations of anthropogenic elements and phosphate \$\pm 1\$ SD \(\$\text{pmol m}^{-3}\$ \), with](#)
 819 [fractional solubility overlaid. There is no phosphate data from Leg 2 \(Black Sea\) as the sampler](#)

820 [malfunctioned on this leg. Bar colours, grey circles and arrows and dashed vertical lines are](#)
821 [described in Figs. 3 & 4. Note that Zn solubility for sample TM39 is affected by contamination of the](#)
822 [t-Zn measurement.](#)

823

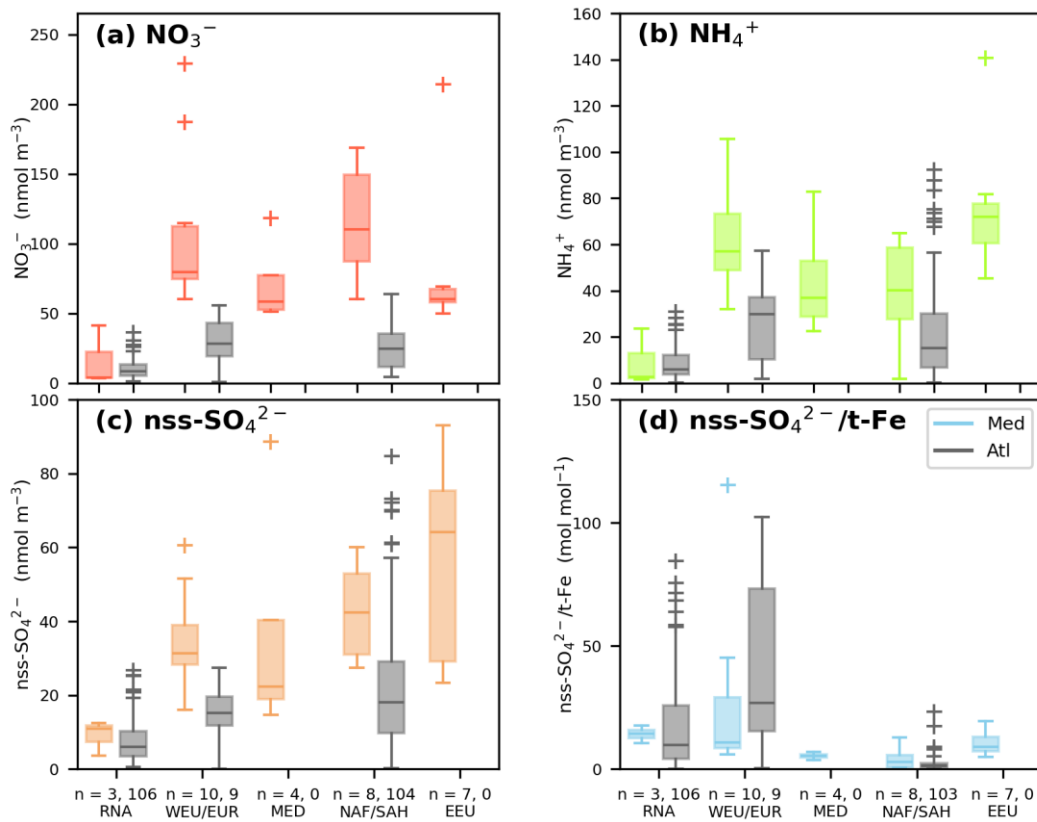


824

825 Figure 7. Log-log plots of fractional solubility plotted against total aerosol concentration (pmol m^{-3})
 826 for primarily lithogenic (left column) and anthropogenic (right column) elements. Samples are colour
 827 coded by air mass, as in previous figures. The grey open symbols show data for RNA, European (EUR)

828 and Saharan (SAH) air mass types over the open Atlantic Ocean from Jickells et al. (2016) for
829 comparison.

830



831

832 Figure 8. Box and whisker plots of aerosol concentrations of (a) NO_3^- , (b) NH_4^+ , (c) nss- SO_4^{2-} (nmol m⁻³)
833 and (d) the molar ratio of nss- SO_4^{2-} to total-Fe from GA04 (coloured boxes) and the Atlantic Ocean
834 (grey boxes; Jickells et al., 2016). Note that WEU and NAF used in this study correspond with EUR
835 and SAH, respectively, from earlier studies from this research group. Crosses indicate outlier values
836 greater than 1.5 times the interquartile range above the upper quartile.